

Spectral Domain Optical Coherence Tomography

Ultra-high Speed, Ultra-high Resolution Ophthalmic Imaging

Teresa C. Chen, MD; Barry Cense, PhD; Mark C. Pierce, PhD; Nader Nassif, BS; B. Hyle Park, PhD; Seok H. Yun, PhD; Brian R. White, BS; Brett E. Bouma, PhD; Guillermo J. Tearney, MD, PhD; Johannes F. de Boer, PhD

Objective: To introduce a new ophthalmic optical coherence tomography technology that allows unprecedented simultaneous ultra-high speed and ultra-high resolution.

Methods: Using a superluminescent diode source, a clinically viable ultra-high speed, ultra-high resolution spectral domain optical coherence tomography system was developed.

Results: In vivo images of the retina, the optic nerve head, and retinal blood flow were obtained at an ultra-high speed of 34.1 microseconds (ms) per A-scan, which is 73 times faster than commercially available optical coherence tomography instruments. Single images (B-scans) consisting of 1000 A-scans were acquired in 34.1 ms, allowing video rate imaging at 29 frames per second with an axial

resolution of 6 μm . Using a different source in a slightly slower configuration, single images consisting of 500 A-scans were acquired in 34 ms, allowing imaging at 29 frames per second at an axial resolution of 3.5 μm , which is 3 times better than commercially available optical coherence tomography instruments. The amount of energy directed into the eye in both cases, 600 μW , is less than that of the Stratus OCT3 and is safe for intrabeam viewing for up to 8 hours at the same retinal location.

Conclusion: Spectral domain optical coherence tomography technology enables ophthalmic imaging with unprecedented simultaneous ultra-high speed and ultra-high resolution.

Arch Ophthalmol. 2005;123:1715-1720

OPTICAL COHERENCE TOMOGRAPHY (OCT) allows noninvasive imaging of ocular structures. Optical coherence tomographic imaging is analogous to B-mode ultrasound imaging, except that it uses light instead of sound.¹ The interface between different ocular tissues can be determined by changes in reflective properties between the tissues. Current experimental ophthalmic OCT instruments provide more structural information than any other ophthalmic diagnostic technique.² With the latest commercially available machine (Stratus OCT3; Carl Zeiss Meditec Inc, Dublin, Calif), axial resolutions of better than 10 μm can be achieved, and cross-sectional retinal images consisting of 512 A-scans can be acquired in 1.28 seconds. Nearly all commercial and research OCT systems developed to date are based on time domain OCT technology (TDOCT). In TDOCT, an individual A-scan is acquired by varying the length of the reference arm in an interferometer, such that the scanned length of the reference arm corresponds to the A-scan length. The main impediment to more widespread clinical use of TDOCT technology is the limited resolution and slow acquisition

time. Simultaneous increases in imaging speed and resolution, without sacrificing image quality, can only be brought about by a fundamentally different approach.

An alternative technology is spectral domain OCT (SDOCT), also known as Fourier domain OCT. In SDOCT, no mechanical scanning of the reference arm is needed. Instead, a spectrum is measured with a spectrometer in the detection arm of the interferometer and converted to depth information by Fourier transformation.³⁻⁵ The detection method using a spectrometer is much more efficient and as a result SDOCT is several orders of magnitude more sensitive than TDOCT.⁶⁻⁸ The higher sensitivity of SDOCT technology allows for detection of weaker signals and for faster data acquisition. A sensitivity improvement of 21.7 dB (150-fold) compared with an equivalent TDOCT system was recently shown.⁹ This has allowed a considerable increase in imaging speed and resolution without compromising image quality¹⁰ and has recently led to in vivo video OCT retinal imaging at 29 frames per second with an axial resolution of 6 μm or 3.5 μm , depending on the light source.^{9,11,12}

Similar to Doppler ultrasound, spectral domain optical Doppler tomography (SDODT) can measure retinal blood flow.

Author Affiliations:
Department of Ophthalmology,
Harvard Medical School,
Boston, Mass (Dr Chen);
Harvard Medical School and
Wellman Center for
Photomedicine, Massachusetts
General Hospital, Boston
(Drs Cense, Pierce, Park, Yun,
Bouma, Tearney, de Boer, and
Messers Nassif and White).

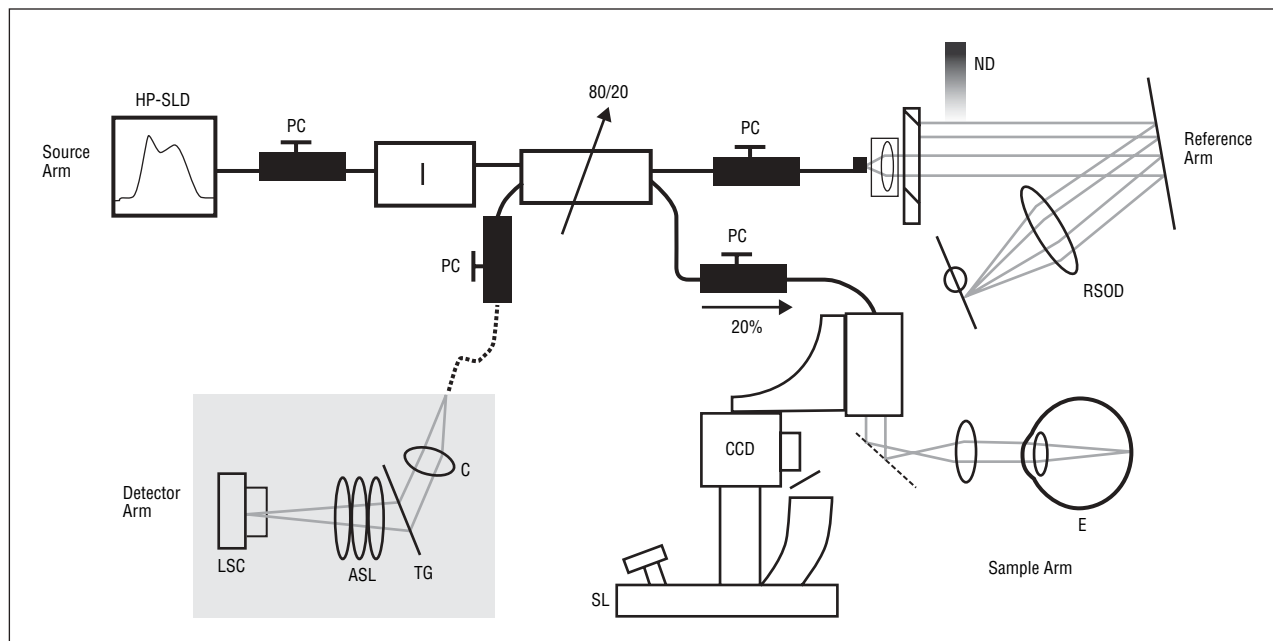


Figure 1. Schematic of the spectral domain optical coherence tomography setup that was used for in vivo measurements. ASL indicates air-spaced lens; C, collimator; CCD, charge-coupled device; E, Eye; HP-SLD, high-power superluminescent diode; LSC, line scan camera; ND, neutral density filter; PC, polarization controllers; RSOD, delay line; SL, slitlamp; TG, transmission grating.

Here we will show several images from the new ultra-high speed, ultra-high resolution superluminescent diode-based SDOCT and SDODT systems. The potential clinical implications of this improved technology will be discussed.

METHODS

PATIENT

The right eye of a 39-year-old Caucasian man was imaged in vivo, using our SDOCT system. The right eye was normal except for being plano - 1.00 × 105°. Best corrected vision was 20/20. Massachusetts Eye and Ear Infirmary and Massachusetts General Hospital institutional review board approval was obtained.

SPECTRAL DOMAIN OPTICAL COHERENCE TOMOGRAPHY

A-scans were acquired at a rate of 29 000 per second (6 μm axial resolution) and 14 500 per second (3.5 μm axial resolution). In **Figure 1**, the experimental setup is shown.⁹⁻¹² The light sources were a commercially available superluminescent diode (SLD) (Superlum Diodes Ltd, Moscow, Russia) with a polarized power of 4.6 mW and a full width at half maximum spectral width of 50 nm centered at 840 nm (6 μm resolution) and an experimental source (BroadLighter; Superlum) with a power of 3.7 mW and a full width at half maximum spectral width in the system of 150 nm centered at 875 nm (3.5 μm resolution). The power incident on the eye was limited to 600 μW, in accordance with the American National Standards Institute maximum permissible exposure for continuous intrabeam viewing.¹³ Light returning from sample and reference arm paths was recombined in the detection arm and sent to a high-speed, high-efficiency spectrometer.^{9,10}

For SDODT, the measured phase stability of our system is more than 25 times better than previously quantified figures

for TDODT systems, and our acquisition speed corresponds to a minimum detectable Doppler shift of ± 25 Hz and a dynamic range of 600, defined as the ratio of maximum to minimum detectable Doppler shift.¹¹ Images were acquired at 29 frames per second (1000 A-lines per frame) and subsequently processed.

The pupil was not dilated for acquisition of any of the images. Because the eyes were not dilated, we did not acquire charge coupled device images of the retina.

RESULTS

Figure 2A shows a horizontal linear scan through the neuroretinal rim and peripapillary retina. **Figure 2B** shows another linear scan through the center of the optic nerve head. **Figure 2A** and **B** were obtained in one twenty-ninth of a second and each consists of 1000 A-scans with an axial resolution of 6 μm. **Figure 3A** shows a horizontal linear scan through the fovea and was acquired in one twenty-ninth of a second and consists of 500 A-scans with an axial resolution of 3.5 μm. For comparison, **Figure 3B** shows a scan of the same area with a source providing 6 μm resolution, showing the improved sharpness of the OCT images at 3.5 μm resolution.

Spectral domain optical Doppler tomography shows a horizontal linear scan through an area inferior to the optic nerve head (**Figure 4**). Blood vessels produce a shadowing effect in underlying regions in the intensity image (**Figure 4A**). In the corresponding phase image (**Figure 4B**), stationary regions are gray, with positive and negative Doppler shifts mapped in black or white, enabling the bidirectional nature of blood flow to be visualized. **Figure 4** was acquired in one twenty-ninth of a second with a resolution of 6 μm. Although not shown in **Figure 4**, pulsatile blood flow can clearly be visualized in real-time in arterioles and venules as small as 10 μm in diameter.¹¹

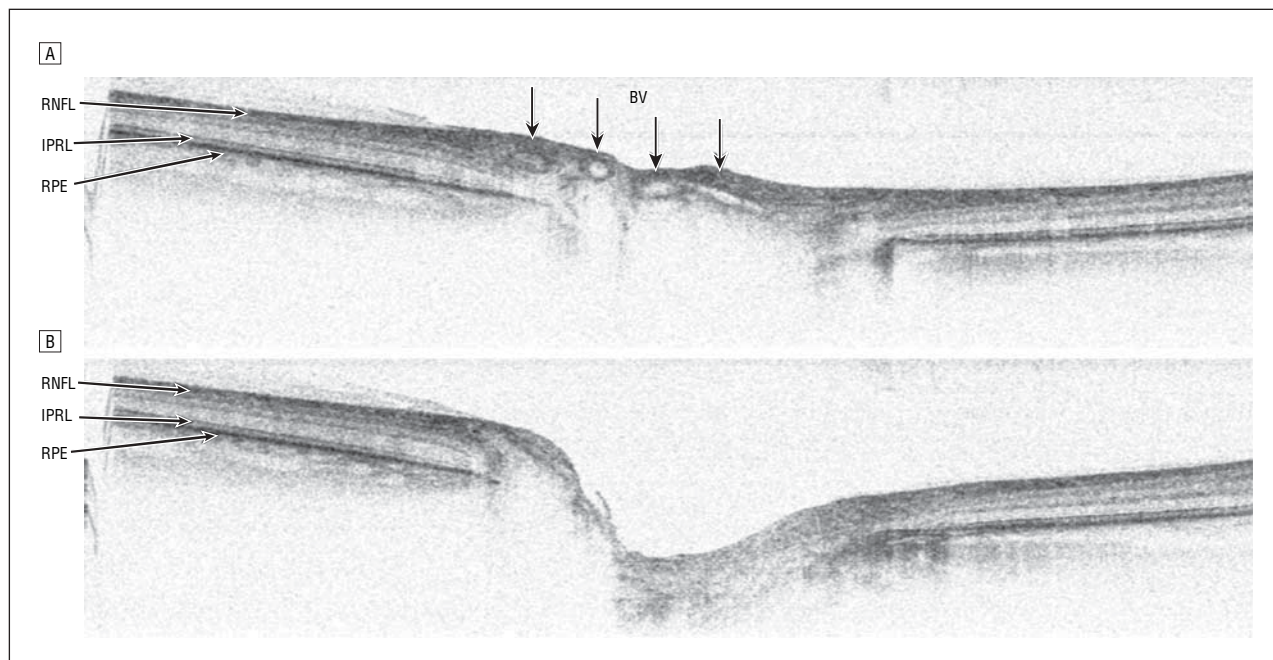


Figure 2. Spectral domain optical coherence tomographic image of the optic nerve and peripapillary region acquired in one twenty-ninth of a second consisting of 1000 A-scans. The image measures 6.1×1.5 mm. A, Horizontal linear scan through the neuroretinal rim and peripapillary retina. B, Linear scan through the center of the optic nerve head. IPRL indicates border between the inner and outer segments of the photoreceptors; RNFL, retinal nerve fiber layer; RPE, retinal pigment epithelium. The choroid and choriocapillaris are shown below. Vertical arrows point toward 4 large blood vessels (BV).

The ultra-high speed imaging capabilities of SD-OCT allow 3-dimensional reconstruction of the optic nerve and peripapillary retina, as shown in **Figure 5**, with this volume assembled from 400 images with an axial resolution of $6 \mu\text{m}$, acquired in a total time of 14 seconds.

COMMENT

Compared with traditional TDOCT, SDOCT technology yields unprecedented acquisition speeds and significantly higher axial resolutions using a potentially affordable SLD source. This system produced high quality images while operating at safe ocular exposure levels, even below that of the commercially available OCT3 system.

Ultra-high resolution TDOCT systems with axial resolutions of less than $3 \mu\text{m}$ have been developed using a titanium-sapphire laser.^{2,14} Although these ultra-broad bandwidths enable axial resolutions better than standard SLD,¹⁴ the principal disadvantage of the current femtosecond titanium-sapphire laser technology is still its high cost and complexity, which currently precludes its widespread clinical use.² A more fundamental limitation of this current ultra-high resolution TDOCT technology is its slow acquisition speed, which is a consequence of the inverse relation between resolution and speed. Although the prototype system had clinically impractical acquisition times of 4 to 12 seconds at an axial scan rate of 50 Hz for a 200 to 600 transverse pixel image, the current system runs at 250 Hz.² In SDOCT, there is no fundamental limiting relation between resolution and speed, and any source can be used without compromising image quality.^{8,10} Superluminescent diodes have been used for commercial OCT imaging systems and the advancement in SLD technology has made available a new

generation of ultra-broad bandwidth light sources that are compact, relatively inexpensive, and require low maintenance. The combination of these new light sources with SDOCT technology has led to in vivo retinal imaging with simultaneous ultra-high axial resolutions and ultra-high speeds.

Spectral domain technology not only offers structural retinal imaging but also allows imaging of retinal blood flow similar to Doppler ultrasound.¹⁵ The flow sensitivity of Doppler OCT greatly depends on the mechanical or phase stability of the OCT system and on how fast images can be taken.^{16,17} Because of the dramatic speed improvement of SDOCT and the absence of moving parts in the reference arm, the phase stability is greatly improved. Spectral domain optical Doppler tomography allows real-time imaging of pulsatile blood flow within blood vessels as small as $10 \mu\text{m}$ and as deep as the choroid.^{11,18}

Spectral domain optical coherence tomography's higher acquisition speeds realistically allow for a shift from 2-dimensional to 3-dimensional (3-D) images of ocular anatomy (Figure 5). For example, a 6.2×6.2 mm area with 62 parallel images $100 \mu\text{m}$ apart can be obtained in 2.1 seconds. Scan areas can be adjusted and scan intervals can be decreased as needed. In glaucoma, instead of only peripapillary circular scans or linear scans, SDOCT scans would allow 3-D mapping of the nerve fiber layer of the entire posterior pole. In diabetic retinopathy,¹⁹ 3-D SDOCT maps of structure and blood flow would show the exact location of clinically significant macular edema and would allow more accurate quantification of macular thickness. In macular degeneration, 3-D maps can delineate the exact extent and depth of choroidal neovascular membranes and may minimize the need for repeat invasive fluorescein angiography. Large choroidal le-

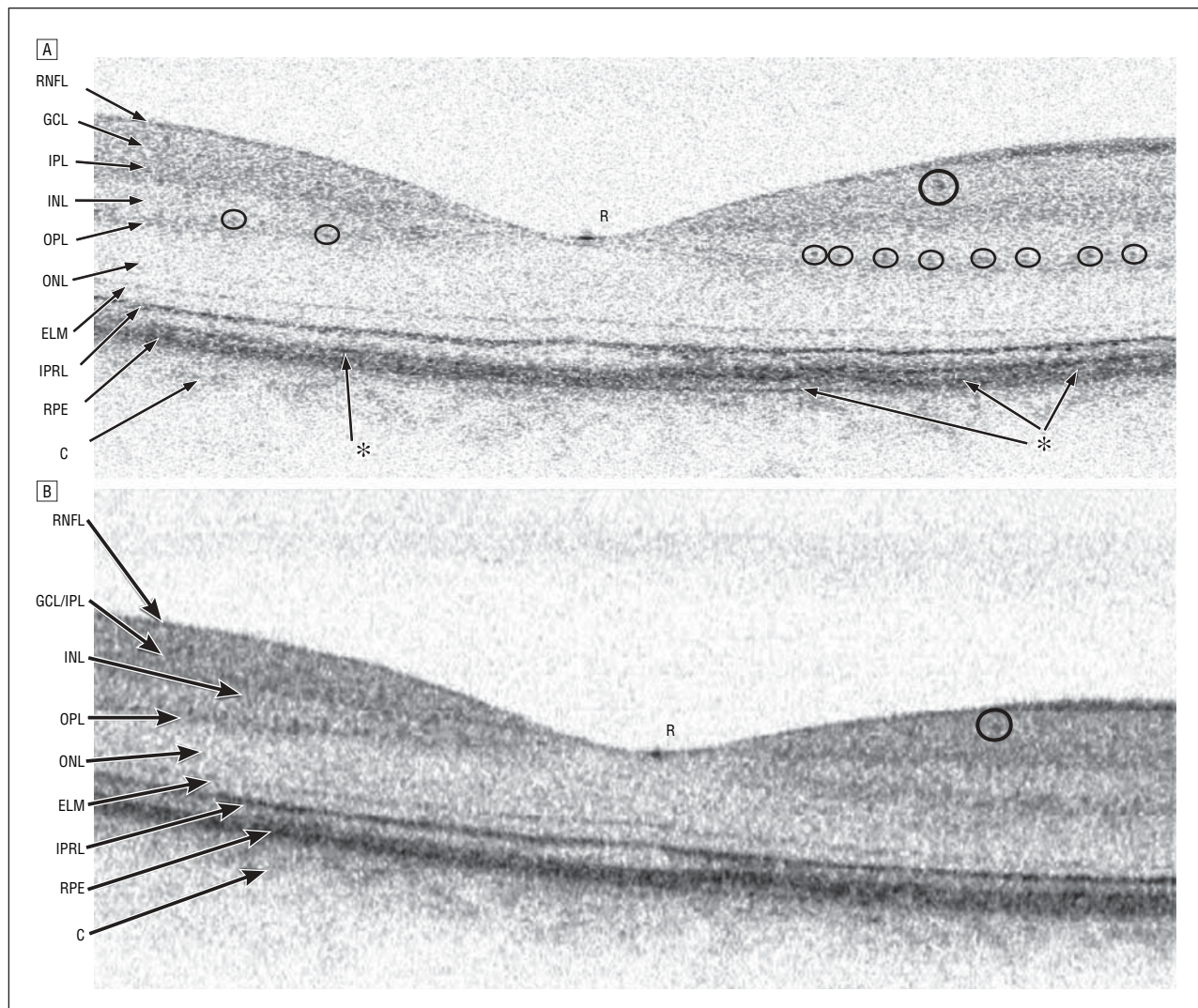


Figure 3. Layers are labeled as follows: RNFL, retinal nerve fiber layer; GCL, ganglion cell layer; IPL, inner plexiform layer; INL, inner nuclear layer; OPL, outer plexiform layer; ONL, outer nuclear layer; ELM, external limiting membrane; IPRL, interface between the inner and outer segments of the photoreceptor layer; RPE, retinal pigment epithelium; C, choriocapillaris and choroid. The blood vessels are circled with darker circles. Structures in the outer plexiform layer are circled with lighter circles. A highly reflective spot in the center of the fovea is marked with an R. A, Ultra-high resolution spectral domain optical coherence tomographic (SDOCT) image of the foveal region acquired in one twenty-ninth of a second consisting of 500 A-scans at a resolution of 3.5 μm . The image measures 3.1 \times 0.61 mm. The image is expanded in the vertical direction by a factor of 2 to provide more detail. Two layers at the location of the RPE at the left and right are marked with arrows and an asterisk. B, Similar image taken with a standard SDOCT system employed with a superluminescent diode. The axial resolution of the image was 6 μm and the image measures 3.2 \times 0.8 mm. The individual layers are less distinct, and structures in the outer plexiform layer are not seen. The differing scattering properties of the RPE are not clearly seen, as in the higher-resolution image.

sions can be mapped, since scans up to 10 mm in width can be obtained quickly with ultra-high resolution. This may allow for better monitoring of posterior intraocular tumors since it affords higher resolution than B-scan ultrasound.²⁰⁻²² Because of SDOCT's ability to create 3-D maps of the retina and to map areas of active blood flow more accurately, this new technology may decrease the need for invasive fluorescein angiography or enable earlier diagnosis of diseases with localized poor blood flow (eg, vasculitis, impending branch retinal vein occlusion, etc).

Spectral domain optical coherence tomography may aid in the management of glaucoma, the second leading cause of blindness in the world.^{23,24} Nerve fiber layer (NFL) assessment is important in glaucoma because it is directly correlated with loss of ganglion cells, which is as-

sumed to be a primary event in glaucomatous damage.²⁵ Since the peripapillary NFL can be on the order of 50 to over 200 μm thick, current resolutions of 10 to 15 μm may not be enough to detect a significant change over time. Therefore, accurate ultra-high resolution SDOCT measurements of NFL thinning may allow for earlier detection and treatment of glaucoma. It has been suggested that NFL thinning may occur as early as 6 years prior to permanent vision loss and may occur prior to clinically detectable optic nerve head changes.²⁶ Spectral domain optical coherence tomography also provides a direct assessment of NFL thickness, unlike scanning laser polarimetry (eg, GDx; Laser Diagnostic Technologies, San Diego, Calif), which indirectly calculates NFL thickness through depth-resolved double-pass phase retardation measurements.²⁷

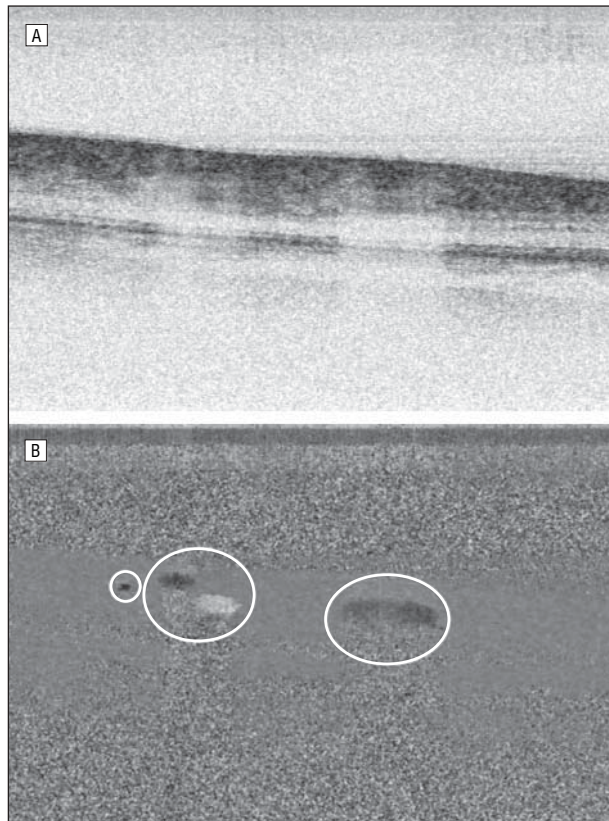


Figure 4. Spectral domain optical Doppler tomography (SDODT) intensity image of the peripapillary retina (A) and corresponding Doppler image which shows bidirectional flow (B) acquired in one twenty-ninth of a second consisting of 1000 A-scans. Image size is 1.6 mm wide \times 1.2 mm deep. In the Doppler image (B), flow is gray scale coded as a positive (white), negative (black), or no Doppler shift (gray). From left to right, the white circles indicate a small vein, an artery-vein pair showing bidirectional flow, and a large vein.

Mapping the true optic nerve head topography is possible with SDOCT (Figure 2 and Figure 5). Previous OCT technologies have not allowed for accurate maps of optic nerve head topography. Even with the ultra-high resolution titanium-sapphire lasers, slower acquisition speeds necessitate realignment of A-scans, which do not allow for evaluation of the true optic nerve head topography.¹⁴ With the ultra-high speeds of SDOCT, realignment of A-scans within a single image becomes unnecessary. Spectral domain optical coherence tomographic maps of optic nerve head topography may provide a better, more objective way to document and monitor progressive glaucomatous changes in the optic nerve head compared with standard disc photography. Spectral domain optical coherence tomography technology is also potentially better than confocal scanning laser ophthalmoscopy techniques (eg, Heidelberg Retina Tomograph II; Heidelberg Engineering, Dossenheim, Germany) in that it is not limited to measuring only surface topography but it also enables higher resolution imaging.

Motion artifacts within a single image become almost negligible with the ultra-high speed nature of SDOCT. Since patient motion artifacts are more of a problem as people become older, the ultra-high speed nature of SDOCT is particularly helpful since some of the most common causes of blindness increase in prevalence as people age (ie, glau-

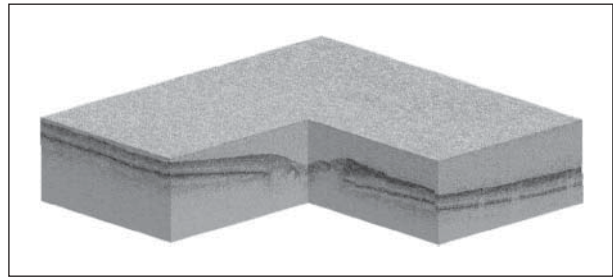


Figure 5. Three-dimensional reconstruction of the optic nerve head and the peripapillary retina, compiled from 400 individual frames mapping out a retinal area 6.2 \times 5 mm, and 1.7 mm in depth. Total acquisition time was 14 seconds.

coma, age-related macular degeneration, and diabetic retinopathy).^{28,29} The ultra-high speed nature of SDOCT also minimizes image distortion caused by involuntary eye movements, although motion artifacts are still present in 3-D volume sets acquired over a few seconds.

Structures not previously visible with conventional TDOCT may be more easily visualized with SDOCT (Figure 2 and Figure 3). Recent studies have also shown that there is a statistically significant difference in the central 5.9 to 6.0 mm macular volume between normal and glaucomatous eyes.³⁰⁻³² Therefore, SDOCT may better enable detection of changes in the macular retinal ganglion cell layer, which is only 4 to 6 cells thick.^{33,34}

In eye diseases where OCT technology has already been shown to be useful,³⁵⁻⁵⁹ further improvements in SDOCT technology may improve the diagnosis and treatment of these many eye diseases, decrease the need for other invasive ophthalmic tests, and enhance understanding of eye disease pathophysiology.

Submitted for Publication: April 9, 2004; final revision received January 3, 2005; accepted January 9, 2005.

Correspondence: Teresa C. Chen, MD, Massachusetts Eye and Ear Infirmary, Glaucoma Service, 243 Charles St, Boston, MA 02114 (teresa_chen@meei.harvard.edu).

Financial Disclosure: Drs Bouma, Tearney, and de Boer have a patent pending.

Funding/Support: This study was supported in part by research grants from the National Institutes of Health (RO1 EY014975 and R24 EY12877). The technical development was supported in part by research grants from the Department of Defense (F4 9620-01-1-0014) and a gift from Dr and Mrs J. S. Chen to the optical diagnostics program of the Wellman Center of Photomedicine.

REFERENCES

1. Fujimoto JG. Optical coherence tomography: introduction. In: Bouma, BE, Tearney, GJ, eds. *Handbook of Optical Coherence Tomography*. New York, NY: Marcel Dekker Inc; 2002:1-40.
2. Drexler W, Sattman H, Hermann B, et al. Enhanced visualization of macular pathology with the use of ultrahigh-resolution optical coherence tomography. *Arch Ophthalmol*. 2003;121:695-706.
3. Fercher AF, Hitzinger CK, Kamp G, Elzaiat SY. Measurement of intraocular distances by backscattering spectral interferometry. *Opt Commun*. 1995;117:43-48.
4. Hausler G, Lindner MW. Coherence radar and spectral radar—new tools for dermatological diagnosis. *J Biomed Opt*. 1998;3:21-31.
5. Wojtkowski M, Leitgeb R, Kowalczyk A, Bajraszewski T, Fercher AF. In vivo human retinal imaging by Fourier domain optical coherence tomography. *J Biomed Opt*. 2002;7:457-463.

6. Mitsui T. Dynamic range of optical reflectometry with spectral interferometry. In: *Japanese Journal of Applied Physics Part 1-Regular Papers Short Notes & Review Papers*. 1999;38:6133-6137.
7. Leitgeb R, Hitzinger CK, Fercher AF. Performance of fourier domain vs time domain optical coherence tomography. *Opt Express*. 2003;11:889-894.
8. De Boer JF, Cense B, Park BH, Pierce MC, Tearney GJ, Bouma BE. Improved signal-to-noise ratio in spectral-domain compared with time-domain optical coherence tomography. *Opt Lett*. 2003;28:2067-2069.
9. Nassif N, Cense B, Park BH, et al. In vivo high-resolution video-rate spectral-domain optical coherence tomography of the human retina and optic nerve. *Opt Express*. 2004;12:367-376.
10. Nassif N, Cense B, Park BH, et al. In vivo human retinal imaging by ultrahigh-speed spectral domain optical coherence tomography. *Opt Lett*. 2004;29:480-482.
11. White BR, Pierce MC, Nassif N, et al. In vivo dynamic human retinal blood flow imaging using ultra-high-speed spectral domain optical Doppler tomography. *Opt Express*. 2003;11:3490-3497.
12. Nassif N, Cense B, Park BH, et al. In vivo human retinal imaging by ultrahigh-speed spectral domain optical coherence tomography. *Opt Lett*. 2004;29:480-482.
13. American National Standards Institute. *American National Standard for Safe Use of Lasers Z136.1*. Orlando, Fla: Laser Institute of America; 2000.
14. Drexler W, Morgner U, Ghanta RK, Kartner FX, Schuman JS, Fujimoto JG. Ultrahigh-resolution ophthalmic optical coherence tomography. *Nat Med*. 2001;7:502-507.
15. Yazdanfar S, Rollins AM, Izatt JA. Imaging and velocimetry of the human retinal circulation with color Doppler optical coherence tomography. *Opt Lett*. 2000;25:1448-1450.
16. Kulkarni MD, van Leeuwen TG, Yazdanfar S, Izatt JA. Velocity-estimation accuracy and frame-rate limitations in color Doppler optical coherence tomography. *Opt Lett*. 1998;23:1057-1059.
17. Zhao YH, Chen ZP, Saxer C, Xiang SH, de Boer JF, Nelson JS. Phase-resolved optical coherence tomography and optical Doppler tomography for imaging blood flow in human skin with fast scanning speed and high velocity sensitivity. *Opt Lett*. 2000;25:114-116.
18. Leitgeb RA, Schmetterer L, Hitzinger CK, et al. Real-time measurement of in vitro flow by Fourier-domain color Doppler optical coherence tomography. *Opt Lett*. 2004;29:171-173.
19. Strom C, Sander B, Larsen N, Larsen M, Lund-Andersen H. Diabetic macular edema assessed with optical coherence tomography and stereo fundus photography. *Invest Ophthalmol Vis Sci*. 2002;43:241-245.
20. Truong SN, Fern CM, Costa DL, Spaide RF. Metastatic breast carcinoma to the retina: optical coherence tomography findings. *Retina*. 2002;22:813-815.
21. Espinoza G, Rosenblatt B, Harbour JW. Optical coherence tomography in the evaluation of retinal changes associated with suspicious choroidal melanocytic tumors. *Am J Ophthalmol*. 2004;137:90-95.
22. Shields CL, Mashayekhi A, Luo CK, Materin MA, Shields JA. Optical coherence tomography in children: analysis of 44 eyes with intraocular tumors and simulating conditions. *J Pediatr Ophthalmol Strabismus*. 2004;41:338-344.
23. The World Bank. *World Development Report*. Oxford, England: Oxford University Press; 1993.
24. Quigley HA. Number of people with glaucoma worldwide. *Br J Ophthalmol*. 1996;80:389-393.
25. Blumenthal EZ, Weinreb RN. Assessment of the retinal nerve fiber layer in clinical trials of glaucoma neuroprotection. *Surv Ophthalmol*. 2001;45(suppl 3):S305-S312.
26. Sommer A, Katz J, Quigley HA, et al. Clinically detectable nerve fiber atrophy precedes the onset of glaucomatous field loss. *Arch Ophthalmol*. 1991;109:77-83.
27. Cense B, Chen TC, Park BH, Pierce MC, de Boer JF. Thickness and birefringence of healthy retinal nerve fiber layer tissue measured with polarization sensitive optical coherence tomography. *Invest Ophthalmol*. 2004;45:2606-2612.
28. Lee PP, Feldman ZW, Ostermann J, Brown DS, Sloan FA. Longitudinal prevalence of major eye diseases. *Arch Ophthalmol*. 2003;121:1303-1310.
29. Congdon NG, Friedman DS, Leitman T. Important causes of visual impairment in the world today. *JAMA*. 2003;290:2057-2060.
30. Greenfield DS, Bagga H, Knighton RW. Macular thickness changes in glaucomatous optic neuropathy detected using optical coherence tomography. *Arch Ophthalmol*. 2003;121:41-46.
31. Guedes V, Schuman JS, Hertzmark E, et al. Optical coherence tomography measurement of macular and nerve fiber layer thickness in normal and glaucomatous human eyes. *Ophthalmology*. 2003;110:177-189.
32. Lederer DE, Schuman JS, Hertzmark E, et al. Analysis of macular volume in normal and glaucomatous eyes using optical coherence tomography. *Am J Ophthalmol*. 2003;135:838-843.
33. Zeimer R. Application of the retinal thickness analyzer to the diagnosis and management of ocular diseases. *Ophthalmol Clin North Am*. 1998;11:359-379.
34. Zeimer R, Asrani S, Zou S, Quigley H, Jampel H. Quantitative detection of glaucomatous damage at the posterior pole by retinal thickness mapping: a pilot study. *Ophthalmology*. 1998;105:224-231.
35. Zolf R, Glacet-Bernard A, Benhamou N, Mimoun G, Coscas G, Soubbrane G. Imaging analysis with optical coherence tomography: relevance for submacular surgery in high myopia and in multifocal choroiditis. *Retina*. 2002;22:192-201.
36. Baba T, Ohno-Matsui K, Yoshida T, et al. Optical coherence tomography of choroidal neovascularization in high myopia. *Acta Ophthalmol Scand*. 2002;80:82-87.
37. Ismail R, Tanner V, Williamson TH. Optical coherence tomography imaging of severe commotio retinae and associated macular hole. *Br J Ophthalmol*. 2002;86:473-474.
38. Uemura A, Uchino E, Doi N, Ohba N. Repair of impending macular hole in the early postoperative period as evaluated by optical coherence tomography. *Arch Ophthalmol*. 2002;120:398-400.
39. Ip MS, Baker BJ, Duker JS, et al. Anatomical outcomes of surgery for idiopathic macular hole as determined by optical coherence tomography. *Arch Ophthalmol*. 2002;120:29-35.
40. Azzolini C, Patelli F, Brancato R. Correlation between optical coherence tomography data and biomicroscopic interpretation of idiopathic macular hole. *Am J Ophthalmol*. 2001;132:348-355.
41. Fujii GY, De Juan E, Bressler NM. Vitrectomy surgery for impending macular hole based on optical coherence tomography. *Retina*. 2001;21:389-392.
42. Kasuga Y, Arai J, Akimoto M, Yoshimura N. Optical coherence tomography to confirm early closure of macular holes. *Am J Ophthalmol*. 2000;130:675-676.
43. Theodossiadis PG, Kollia AK, Gogas P, Panagiotidis D, Moschos M, Theodossiadis GP. Retinal disorders in preclampsia studied with optical coherence tomography. *Am J Ophthalmol*. 2002;133:707-709.
44. Stanga PE, Downes SM, Ahuja RM, et al. Comparison of optical coherence tomography and fluorescein angiography in assessing macular edema in retinal dystrophies: preliminary results. *Int Ophthalmol*. 2001;23:321-325.
45. Neubauer AS, Priglinger S, Ullrich S, et al. Comparison of foveal thickness measured with the retinal thickness analyzer and optical coherence tomography. *Retina*. 2001;21:596-601.
46. Hirakawa H, Iijima H, Gohdo T, Tsukahara S. Optical coherence tomography of cystoid macular edema associated with retinitis pigmentosa. *Am J Ophthalmol*. 1999;128:185-191.
47. Antcliff RJ, Ffytche TJ, Shilling JS, Marshall J. Optical coherence tomography of melanocytoma. *Am J Ophthalmol*. 2000;130:845-847.
48. Fukasawa A, Iijima H. Optical coherence tomography of choroidal osteoma. *Am J Ophthalmol*. 2002;133:419-421.
49. Muscat S, Srinivasan S, Sampat V, Kemp E, Parks S, Keating D. Optical coherence tomography in the diagnosis of subclinical serous detachment of the macula secondary to a choroidal nevus. *Ophthalmic Surg Lasers*. 2001;32:474-476.
50. Hassenstein A, Bialasiewicz AA, Richard G. Optical coherence tomography in uveitis patients. *Am J Ophthalmol*. 2000;130:669-670.
51. Antcliff RJ, Stanford MR, Chauhan DS, et al. Comparison between optical coherence tomography and fundus fluorescein angiography for the detection of cystoid macular edema in patients with uveitis. *Ophthalmology*. 2000;107:593-599.
52. Bek T, Kandi M. Quantitative anomaloscopy and optical coherence tomography scanning in central serous chorioretinopathy. *Acta Ophthalmol Scand*. 2000;78:632-637.
53. Iida T, Hagimura N, Sato T, Kishi S. Evaluation of central serous chorioretinopathy with optical coherence tomography. *Am J Ophthalmol*. 2000;129:16-20.
54. Muscat S, McKay N, Parks S, Kemp E, Keating D. Repeatability and reproducibility of corneal thickness measurements by optical coherence tomography. *Invest Ophthalmol Vis Sci*. 2002;43:1791-1795.
55. Hoerauf H, Scholz C, Koch P, Engelhardt R, Laqua H, Birngruber R. Transscleral optical coherence tomography: a new imaging method for the anterior segment of the eye. *Arch Ophthalmol*. 2002;120:816-819.
56. Nozaki M, Kimura H, Kojima M, Ogura Y. Optical coherence tomographic findings of the anterior segment after nonpenetrating deep sclerectomy. *Am J Ophthalmol*. 2002;133:837-839.
57. Wirbelauer C, Scholz C, Hoerauf H, Pham DT, Laqua H, Birngruber R. Noncontact corneal pachymetry with slit lamp-adapted optical coherence tomography. *Am J Ophthalmol*. 2002;133:444-450.
58. Ko TH, Fujimoto JG, Duker JS, et al. Comparison of ultrahigh- and standard-resolution optical coherence tomography for imaging macular hole pathology and repair. *Ophthalmology*. 2004;111:2033-2043.
59. Apushkin MA, Fishman G, Janowicz MJ. Monitoring cystoid macular edema by optical coherence tomography in patients with retinitis pigmentosa. *Ophthalmology*. 2004;111:1899-1904.